Transfer-matrix study of the staggered body-centered solid-on-solid model

Enrico Carlon*
Instituut voor Theoretische Fysica, Universiteit Utrecht, Postbus 80006, 3508 TA Utrecht, The Netherlands and Höchstleistungsrechenzentrum, Forschungszentrum Jülich, D-52425 Jülich, Germany

Giorgio Mazzeo
Dipartimento di Fisica, Università di Genova, and Istituto Nazionale per la Fisica della Materia (INFM), via Dodecaneso 33, 16146 Genova, Italy

Henk van Beijeren
Instituut voor Theoretische Fysica, Universiteit Utrecht, Postbus 80006, 3508 TA Utrecht, The Netherlands and Höchstleistungsrechenzentrum, Forschungszentrum Jülich, D-52425 Jülich, Germany

(Received 16 May 1996; revised manuscript received 13 September 1996)

The phase diagram of the staggered six vertex, or body-centered solid-on-solid model, is investigated by transfer-matrix and finite-size scaling techniques. The phase diagram contains a critical region, bounded by a Kosterlitz-Thouless line, and a second-order line describing a deconstruction transition. In part of the phase diagram the deconstruction line and the Kosterlitz-Thouless line approach each other without merging, while the deconstruction changes its critical behavior from Ising-like to a different universality class. Our model has the same type of symmetries as some other two-dimensional models, such as the fully frustrated XY model, and may be important for understanding their phase behavior. The thermal behavior for weak staggering is intricate. It may be relevant for the description of surfaces of ionic crystals of CsCl structure. [S0163-1829(97)05001-7]

I. INTRODUCTION

Six vertex models were introduced by Slater[1] to describe ferroelectricity in two-dimensional networks. Placing arrows on the bonds of a square lattice one can define the 16 possible arrangements of arrows pointing towards and away from a lattice point as vertices. In six vertex models only those six vertex configurations are kept (see Fig. 1) that satisfy the *ice rule*, i.e., they have two arrows pointing in and two pointing out at each vertex. Assigning energies $\epsilon_1, \ldots, \epsilon_6$ to these vertices one obtains a class of exactly solved models.[2,3]

Six vertex models can also be interpreted as surface models, by mapping them to the so-called body-centered solid-on-solid (BCSOS) models,[4] defined as limiting cases of a lattice gas, or Ising model, on a body-centered-cubic lattice. Therefore the phase structure of the six vertex model as function of its vertex weights can be translated directly to the surface phase structure of the corresponding BCSOS model. The mapping turned out to be important in understanding the properties of the *roughening transition*.[5] Using the exact solution of the six vertex model it was found that roughening is a transition of infinite order of the Kosterlitz-Thouless (KT) type, confirming previous renormalization-group results.[6]

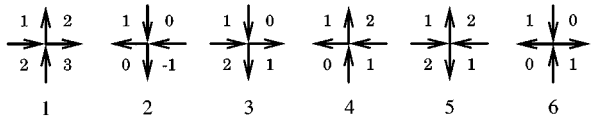

FIG. 1. The six vertices and the corresponding height configurations.

Experimental situations often are too complex to allow even a qualitative description by the exactly solved BCSOS models. Various extensions of the standard six vertex model have been proposed to deal with these cases. Two main classes may be identified: one where interactions between vertices are added, and another one in which the vertex lattice is split into two sublattices with different vertex energies. These modifications, however, lead to models which, apart from some particular cases,[7,8] lose the property of being exactly solvable. Other techniques (e.g., numerical ones) have to be adopted. Models in the first class have been proposed to account for further neighbor interactions between surface atoms, which may change the symmetry of the ground state and give rise to phase transitions other than the roughening transition. Vertex interactions were introduced to reproduce the (2×1) reconstruction of the (110) face of fcc noble metals like Au and Pt.[9] This led to investigations on equilibrium phase transitions on these surfaces as well as on surfaces of lighter metals like Ag, Rh, etc.[10] A model of the (100) surface of an fcc crystal exhibiting a (2×2) reconstructed ground state[11] has recently extended the list. The second class of models, with vertex weights alternating on the two sublattices, are known as *staggered six vertex models*. A staggering only involving the weights of vertices 5 and 6 corresponds to the imposition of a ''staggered field,'' i.e., a field coupled to the arrow directions that changes sign between neighboring arrows. This gives rise to an inverse roughening transition in part of the phase diagram.[12] Alternating the values for the energies of the vertices 1, 2 and 3, 4 on the two sublattices leads to a model known as ''the staggered six vertex model'' (or staggered BCSOS model) in the

literature. In a large part of its parameter space it can be mapped onto the Ashkin-Teller model.[13] Using this transformation Knops investigated the phase structure of the staggered BCSOS model in part of its phase diagram by renormalization-group methods,[14] but until recently a large region of the phase diagram has remained unexplored.

In this paper we present a complete account of our investigations, over the full range of parameters, of the staggered BCSOS model. A preliminary description has been given already in Ref. 15, here we present further details as well as a number of different results.

In the unexplored region of the phase diagram the model has a ground state which is twofold degenerate, therefore it has a symmetry of Ising type. The twofold degeneracy is lost at a second-order transition line which approaches another line of KT roughening transitions. The interplay between the two is particularly interesting, especially since a similar interplay between a KT and a second-order transition has been found for several different models, among which other models for reconstructed surfaces,[10,16] but also the fully frustrated XY model[17–19] and coupled XY-Ising models.[20,21] They have received a great deal of attention in recent years and till now their critical behavior is not fully understood. The strong interplay between Ising and KT degrees of freedom may lead to several possible scenarios where, in a certain region of the phase diagram, either the two transitions occur close to each other but remain separate, or they merge into a single phase transition, which may perhaps belong to a new universality class.

Apart from these more theoretical aspects the model is likely to be relevant for the study of the equilibrium properties of a certain class of crystal surfaces, e.g. the (001) surface of ionic crystals of the CsCl structure. This too will be discussed in some detail.

The paper is structured as follows. In Sec. II we give a description of the model. In Sec. III we present its full phase diagram. In Sec. IV we review the techniques employed in our studies, i.e., the transfer-matrix method and finite-size scaling, and discuss the correlation functions and free energies we calculated to derive our results. In Sec. V we discuss the critical exponents of the model and some possible scenarios for the changes in the critical behavior along the deconstruction line. In Sec. VI we conclude with a brief discussion of related models.

II. THE STAGGERED SIX VERTEX MODEL

The partition function of the six vertex model is given by

$$Z=\sum_{\{\mathcal{C}\}} e^{-\beta\sum_{i=1}^{6} n_i(\mathcal{C})\epsilon_i}, \tag{1}$$

where the sum runs over the set of all allowed vertex configurations $\{\mathcal{C}\}$ and $n_i(\mathcal{C})$ denotes the number of vertices of type i in the configuration $\mathcal{C}$ ($\beta=1/k_BT$, with k_B being the Boltzmann's constant and T being the temperature). The model has been solved exactly[22,2,3] for any choice of values of the energies ϵ_i ($i=1\ldots6$). A relatively simple choice of the vertex energies is given by $\epsilon_1=\epsilon_2=\epsilon_3=\epsilon_4=\epsilon$ and $\epsilon_5=\epsilon_6=0$ which defines, for $\epsilon>0$, the so-called F model. The ground state is twofold degenerate and is composed of vertices 5 and 6 arranged alternatingly in a chessboard configuration. The low-temperature phase is usually called an ''antiferroelectric'' phase, since along both horizontal and vertical rows the arrows predominantly alternate in direction. From the exact solution it is known that this system undergoes an infinite order phase transition to a disordered paraelectric state at $\beta\epsilon=\ln 2$.

As already pointed out in the Introduction, the six vertex models are isomorphic to a class of solid-on-solid (SOS) models called BCSOS models.[4] Microscopic configurations of an SOS model are given in terms of discrete heights h_i of surface atoms with respect to a reference plane. All lattice sites up to these heights are occupied and all sites above them are empty. In the BCSOS model the height variables are placed on the dual lattice of the six vertex lattice. This is subdivided into an even and an odd sublattice, which are intertwined in a chessboard pattern and on which the surface heights assume even, respectively, odd values only. The even sites will be referred to as black (B) sites and the odd ones as white (W) sites. In addition the height differences between neighboring sites are restricted to the values ±1. The mapping of six vertex configurations to corresponding configurations of a BCSOS model is very simple. The height differences between neighboring sites are put in a one-to-one correspondence with the arrow directions in the six vertex configuration. The convention is that the higher of the two surface sites is at the right side of the arrow. Given a configuration of vertices, the configuration of heights is fixed uniquely once the height of a reference atom has been fixed (see Fig. 1).

The vertex energies can be reinterpreted in terms of bond energies between the atoms. When periodic boundary conditions are applied along the (say) horizontal direction of the vertex lattice the number of vertices 5 and 6 per row is equal, therefore with no loss of generality one can always choose $\epsilon_5=\epsilon_6=0$, fixing the point of zero energy. The vertices 5 and 6 describe local configurations in which the height variables on either diagonal are equal (see Fig. 1). Vertices 1, 2, 3, and 4 correspond to configurations where the height variables along either of the two diagonals are different, therefore ϵ_1, ϵ_2, ϵ_3, and ϵ_4 can be viewed as energies needed to break a next-nearest-neighbor bond and produce a height difference of two vertical lattice units between neighboring sites of equal color.

In the ordinary BCSOS model the distinction between B and W atoms has been introduced only for convenience of description, but the two sublattices are equivalent and are treated exactly on the same footing. Knops[14] extended the model to a two-component system where the B and W atoms are physically different. While energy zero is still attributed to all vertices 5 and 6, Knops assigned two different energies, ϵ and ϵ', to broken bonds between W-W and B-B atoms, respectively. In terms of the six vertex representation also the vertex lattice is divided into two alternating sublattices I and II on which the vertices assume different energies as follows:

$$\begin{cases} \text{on sublattice I:} & \epsilon_1=\epsilon_2=\epsilon;\epsilon_3=\epsilon_4=\epsilon';\epsilon_5=\epsilon_6=0 \\ \text{on sublattice II:} & \epsilon_1=\epsilon_2=\epsilon';\epsilon_3=\epsilon_4=\epsilon;\epsilon_5=\epsilon_6=0. \end{cases} \tag{2}$$

This choice defines the staggered six vertex model. In the BCSOS representation the model is described by the Hamiltonian:

$$H=\frac{\epsilon}{2}\sum_{\langle ij\rangle}|h_i^W-h_j^W|+\frac{\epsilon'}{2}\sum_{\langle kl\rangle}|h_k^B-h_l^B|, \tag{3}$$

subject to the constraint that the height difference between neighboring B and W sites is ± 1. The first sum in Eq. (3) runs over all pairs of neighboring W sites on the surface and the second sum over the corresponding B pairs. Throughout this article we will also use the parameter δ, defined by the relation $\epsilon'=\epsilon+2\delta$. As mentioned already in the Introduction the model defined here will be referred to as the staggered six vertex (or BCSOS) model. Obviously when $\epsilon=\epsilon'$ ($\delta=0$) one recovers the usual F model.

For negative values of the vertex energies ϵ and ϵ', the system may model ionic crystals of bcc structure as, for instance, CsCl.[23] The constraint of minimal height difference between neighboring surface sites reflects the effects of the strong attraction between oppositely charged ions, while neighboring pairs of the same color, having equal charges, repel each other. It is further assumed that on top of the Coulombic repulsion other interactions, as for instance spin exchange, generate a slight difference in the energies for broken bonds between B-B and W-W pairs ($\epsilon\neq\epsilon'$). In the staggered BCSOS model the interaction range is limited to next-nearest neighbors and to have a more realistic representation of ionic crystals one needs to extend the interactions to further neighbors. Yet we expect the phase structure described here for the staggered BCSOS model may be encountered in real ionic crystals.

III. THE PHASE DIAGRAM

We have investigated the phase diagram of our model by means of transfer-matrix and finite-size scaling techniques, which will be the subject of Sec. IV. Here we present the main results. Since the model shows a trivial symmetry upon exchange of ϵ and ϵ', corresponding to the replacement $(\delta,\epsilon)\leftrightarrow(-\delta,\epsilon+2\delta)$, we can restrict ourselves to the region $\delta\geqslant 0$. The phase diagram naturally divides into three sectors of globally different behavior, though smoothly connected to each other. These are described in the three following subsections.

A. The range $\epsilon>0;\epsilon'>0$

For positive values of ϵ and ϵ' Knops[14] investigated the phase diagram through a mapping onto the Ashkin-Teller model;[13] the phase diagram of the latter had been obtained before by renormalization-group methods.[24] On the $\beta\epsilon$ axis the (001) surface in the corresponding BCSOS model is in a flat phase for $\beta\epsilon>\ln 2$, whereas the interval $\beta\epsilon\leqslant\ln 2$ represents the temperature region in which the surface is rough. The infinite order transition occurring at the KT point $\beta\epsilon=\ln 2$, $\beta\delta=0$ corresponds to the roughening transition of this surface.

Roughening is a phase transition which can be characterized by the vanishing of the free energy of a *step*, separating two surface regions of different average height. The roughening transition results into a proliferation of steps leading to a delocalization of the surface position and to a logarithmic divergence of the mean square height difference at large distances:

$$G(R_{ij})=\langle(h_i-h_j)^2\rangle\sim 2a_V^2K(T)\ln R_{ij}$$
$$\text{for } R_{ij}\to\infty \text{ and } T\geqslant T_R \tag{4}$$

with a_V being the vertical lattice spacing; $K(T)$ is a temperature-dependent prefactor, R_{ij} is the distance between the lattice sites i and j, and T_R is the roughening temperature. Below T_R, $G(R)$ saturates for large R at a temperature-dependent constant value. Renormalization-group calculations[25] show that at T_R the prefactor assumes the universal value

$$K(T_R)=\frac{1}{\pi^2}. \tag{5}$$

In the particular case of the exactly solved F model, $K(T)$ is known for every temperature above T_R,[26] that is

$$K(T)=\frac{1}{\pi\arccos\Delta}, \tag{6}$$

where $\Delta=1-e^{2\beta\epsilon}/2$. In fact Eqs. (4) and (6) are valid not only in the high-temperature phase of the F model, but also for $\delta=0$, $\beta\epsilon<0$, which defines the so-called inverted F model:[2,12] all along the negative $\beta\epsilon$ axis the surface is in a rough state.

For $\delta\neq 0$ Knops found two critical lines originating from the KT point and running into the regions $\delta>0$ and $\delta<0$. The lines represent phase transitions of the Ising type from an ordered low-temperature phase to a disordered flat (DOF) phase, similar to the phase introduced by Rommelse and Den Nijs.[27]

The ground state of the model is twofold degenerate. At higher temperatures the more weakly bound sublattice fluctuates above and below the more strongly bound sublattice, which remains almost localized at a given level. In the limit $\delta\to\infty$ the model can be mapped *exactly* onto the two-dimensional Ising model, which is critical at $\beta\epsilon=\ln(1+\sqrt{2})$; the strong sublattice is ''frozen'' to height (say) zero, the only freedom left for the heights of the other sublattice is to take the values ± 1 just below or above that of the strong sublattice (see Fig. 2). According to the renormalization-group results obtained for the Ashkin-Teller model[24] the phase transition remains in the universality class of the two-dimensional Ising model all along the critical line down to $\delta=0$.

Starting from the low-temperature phase and increasing the temperature, the system undergoes an Ising transition to the DOF phase, while roughening is pushed up to infinite temperature.[14] We reinvestigated this part of the phase diagram with the transfer-matrix methods to be described in Sec. IV and obtained results in full agreement with those of Knops.

B. The range $\epsilon<0;\epsilon'>0$

When ϵ becomes negative the ground state of the system changes drastically (irrespective of the sign of ϵ'). Breaking bonds between white atoms now lowers the energy, so that at

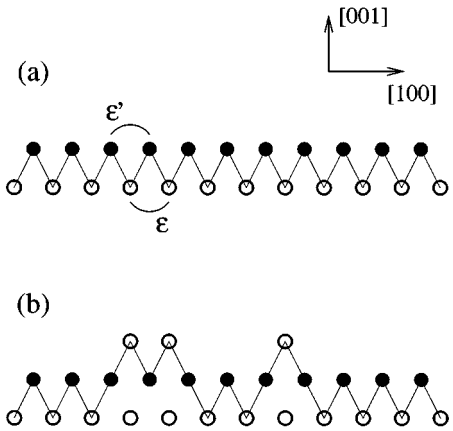

FIG. 2. Side view of the surface for $\epsilon>0$ in one of its ground states (a) and in the Ising limit $\beta\delta\to\infty$ at a finite value of temperature (b). In the ground state atoms form uninterrupted rows also in the [010] direction (orthogonal to the page). The structure of the DOF phase resembles that of (b), with broken bonds between B atoms always less frequent than between W atoms (their energies are ϵ',ϵ respectively, with $\epsilon'>\epsilon>0$). In the figure, ϵ and ϵ' denote bonds the breakage of which would cost these amounts of energy.

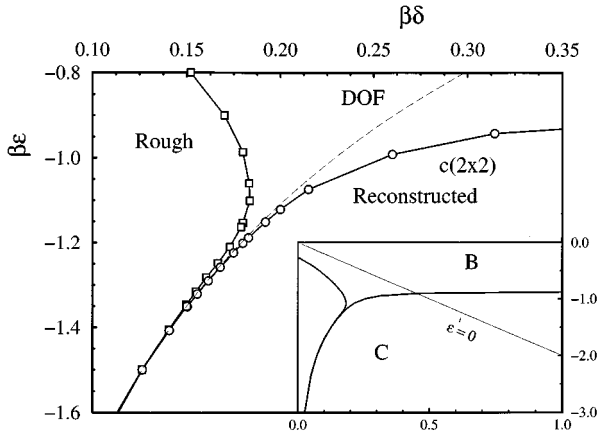

FIG. 4. The phase diagram of the staggered BCSOS model. We show here only the sector C, and part of the sector B in the inset. Open circles denote the deconstruction line and open squares the roughening line. The estimate for the roughening condition, provided by Eq. (9), is shown as a dashed line. It is almost indistinguishable from the correct curve (squares) for $\beta\epsilon\lesssim-1.3$.

zero temperature one finds the black sublattice unbroken (provided $\delta>0$), while atoms of the white sublattice are found alternatingly above and below the black sublattice (see Fig. 3). This surface configuration is commonly referred to as a $c(2\times2)$ reconstructed surface. In the equivalent six vertex representation the ground state is formed by columns of vertical arrows running alternately all upwards and all downwards, and by rows of horizontal arrows running alternately all right and all left. Such an arrangement of directed paths is known as the *Manhattan lattice*, due to its resemblance to the one-way street pattern of Manhattan. As the energy is invariant under the reversal of all arrows, the ground state is twofold degenerate, just as in the case $\epsilon>0$. Indeed in the limit $\delta\to\infty$ the model can be mapped *exactly* onto an antiferromagnetic Ising model leading to the value $\beta\epsilon=-\ln(1+\sqrt{2})$ for the critical temperature. This constitutes a horizontal asymptote, as in the case $\epsilon>0$, for a second-order transition line, whose existence can be deduced again from the mapping of the staggered six vertex model onto the Ashkin-Teller model.[28] It separates a low-temperature $c(2\times2)$ reconstructed phase from a high-temperature DOF phase, where the reconstruction order is lost but the surface is still globally flat: it is the same DOF phase found for $\epsilon>0$; no singularities are met in crossing the $\beta\delta$ axis. Our transfer-matrix calculations confirm the existence of this critical line and show it exhibits Ising-type critical behavior throughout sector B.

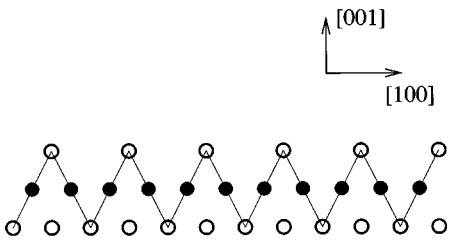

FIG. 3. Side view of one of the ground states of the model for $\epsilon<0$. Notice that W atoms alternate in height with respect to the B sublattice also in the [010] direction (orthogonal to the page).

C. The range $\epsilon<0;\epsilon'<0$

For $\epsilon'<0$ the mapping of the staggered six vertex model to the Ashkin-Teller model leads to negative Boltzmann weights in the latter. It loses its physical relevance and cannot be used any more to make predictions on the phase behavior of the staggered six vertex model. In spite of this Kohmoto *et al.*[28] have made some conjectures, which have proven to be correct, on the physical situation beyond the ''horizon'' $\epsilon+2\delta=0$.

Our transfer-matrix analysis shows the existence of three phases: a low-temperature $c(2\times2)$ reconstructed phase and a DOF phase, which are present already in sector B, and a rough phase, which is found only in the present sector. Two critical lines separate these phases, as shown in Fig. 4: the first one is just the continuation of the second-order line beyond the horizon. It still separates the $c(2\times2)$ region from the DOF region and asymptotically approaches the axis $\beta\delta=0$. We have strong indications that, within at least a major part of the sector $\epsilon'<0$, this line does not belong to the Ising universality class. We will present the evidence for this in Sec. V. The other critical line is a line of KT points separating the rough region (or *critical fan*, as predicted already by Kohmoto *et al.*[28]) from the DOF region.

The point where the KT line meets the vertical axis can be determined from the exact solution of the F model as the point where the prefactor of the logarithmic term in the mean-square height difference is four times as large as its universal value assumed at the ordinary roughening temperature of the F model

$$K(T)=4K(T_R)=\frac{4}{\pi^2}, \tag{7}$$

from which one obtains, inverting Eq. (6):

$$\beta\epsilon=\frac{1}{2}\ln(2-\sqrt{2})\approx-0.2674. \tag{8}$$

The factor four in Eq. (7) stems from the fact that for $\delta\neq 0$ the roughening transition is driven by steps of a height of two vertical lattice units (as in Ref. 12), due to the inequivalence between the two atomic sublattices.

A simple estimate of the roughening transition temperature based on a random-walk approximation (see Ref. 15) yields

$$e^{-2\beta\delta}+e^{\beta\epsilon}=1. \tag{9}$$

This line has been drawn in Fig. 4. Indeed, for large and negative $\beta\epsilon$ it is seen to run very close to the KT line, which we could determine with great accuracy by the methods described in the next section.

A most remarkable feature of our phase diagram is the apparent merging of the second-order and the KT line into a single line (see Fig. 4). Their horizontal distance d as a function of $\beta\epsilon$ can be well described by a curve of the form $d(\beta\epsilon)=Ce^{\alpha(\beta\epsilon)}$, with $\alpha\simeq 12$.[15] This exponential fit suggests that although the two lines are coming rapidly closer together as $\beta\epsilon$ is decreasing, they do never actually merge. Other fits, of the form $d(\beta\epsilon)=C|\beta\epsilon-\beta\epsilon_0|^{\alpha}$, which would be expected to work in the case of a merging of the lines at $\epsilon=\epsilon_0$, could not be stabilized against changes in the fitting range.

The apparent noncrossing of the two critical lines at first looks very surprising. At low temperatures a domain wall between two different Ising phases mainly consists of diagonal sequences of vertices 5 and 6, as depicted in Fig. 5; its energy per unit length approximately equals $-\epsilon/\sqrt{2}$. On the other hand a step consists mainly of long horizontal and vertical chains of overturned arrows and has an approximate energy per unit length of 2δ. To a first approximation steps do not couple with the Ising order, since the reconstructed phase remains the same at both sides of the step (see Fig. 6). Hence one would expect the KT line (characterized by vanishing step free energy) and the Ising line (vanishing Ising domain-wall free energy) to cross near $\epsilon+2\sqrt{2}\delta=0$. We think that the actual noncrossing of the two lines can be explained as follows. When temperature is raised, more and more closed steps will be formed on the surface as one approaches the roughening temperature T_R. On these steps the direction of the arrows is reversed. In this way the Ising order parameter becomes more and more diluted, which will, eventually, strongly reduce the free energy of a domain wall. If in the end the closed steps become so prolific that they cover on average half of the surface, without becoming of infinite length, the Ising order disappears without roughening of the surface.

For $2\delta\lesssim 0.4|\epsilon|$ the thermal behavior implied by our phase diagram is quite intricate and remarkable. At low temperatures the surface is in a $c(2\times 2)$ reconstructed flat phase, then on raising the temperature there is a second-order transition to a DOF phase, rapidly followed by a KT transition to a rough phase. Next there is a reentrant KT transition to the DOF phase. This is an inverted roughening transition similar to the one described in Ref. 12. Finally, as temperature approaches infinity, the system asymptotically approaches a rough phase again. Instead for $2\delta\gtrsim 0.4|\epsilon|$ the system goes through a single phase transition from the ordered to a DOF phase and remains flat for all finite temperatures.

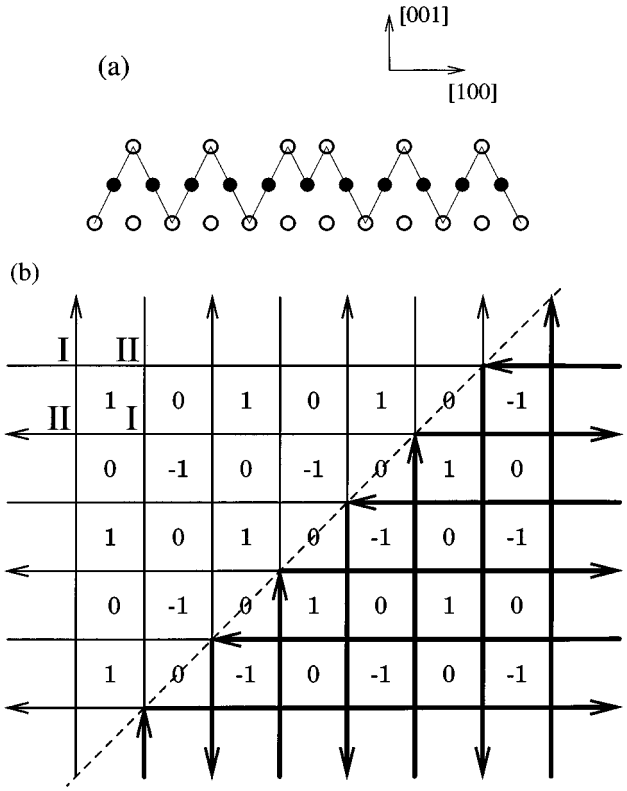

FIG. 5. A domain wall separating two different Ising phases for $\epsilon<0$, (a) in side view and (b) seen from above in the vertex lattice.

IV. TRANSFER-MATRIX AND FINITE-SIZE SCALING METHODS

Transfer-matrix techniques are frequently used in studies of the critical properties of two-dimensional systems with short-range interactions. The construction of the transfer matrix (TM) follows a standard procedure and the interested reader is referred to the existing literature[3] for details.

We use two different transfer matrices, one oriented parallel to the axes of the vertex lattice and another one tilted over 45° with respect to these axes. We refer to the former as *vertical* TM and to the latter as *diagonal* TM (Fig. 7 shows a configuration of the diagonal TM). We consider a lattice of

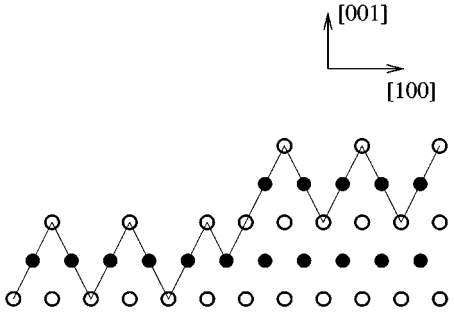

FIG. 6. Side view of a (double height) step as an excitation of the Manhattan ground state.

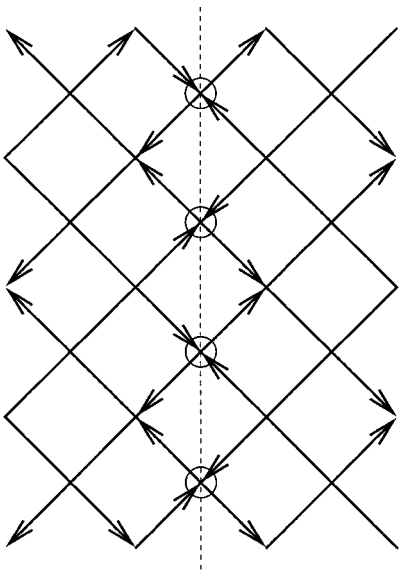

FIG. 7. Part of a ground-state configuration of an $N\times\infty$ system with N odd. Due to partial frustration, the system produces a domain wall made of a sequence of vertices 5 and 6 (denoted by circles).

width N and height M, with periodic boundary conditions in the horizontal direction. For the vertical TM the subdivision of the lattice into a white and a black sublattice, combined with the periodic boundary conditions, restricts N to even values. For the diagonal TM the horizontal and vertical axis are chosen along the diagonals of the vertex lattice and N can be odd as well as even. The element T_{ij} of the matrix is defined as the Boltzmann weight of a row of N vertices generated by arrow configurations labeled by the indices i and j. One has $T_{ij}=0$ if this row of vertices does not satisfy the ice rule. For the vertical TM, if i and j are identical there are in fact two possible configurations of rows of vertices: in this case the transfer-matrix simply sums their Boltzmann weights.

There are 2^N different arrow configurations for the vertical TM, whereas for the diagonal TM this number is 2^{2N}. The largest values of N we could treat numerically were $N=22$ for the vertical and $N=12$ for the diagonal TM. Actually, due to the rotation of the lattice over 45° the latter should be compared to $12\sqrt{2}\approx 17$ for the vertical TM.

In the limit $M\to\infty$ the partition function per row becomes

$$\lim_{M\to\infty}(Z_{N\times M})^{1/M}=\lambda_0(N) \tag{10}$$

with $\lambda_0(N)$ the largest eigenvalue of T, from which the free energy per row follows as

$$\beta f(N)=-\ln\lambda_0(N). \tag{11}$$

To each state i we associate a polarization $P_i=N_{i\uparrow}-N_{i\downarrow}$, with $N_{i\uparrow}$ and $N_{i\downarrow}$ the total numbers of up and down[29] arrows in the state i. By virtue of the periodic boundary conditions in the horizontal direction the transfer matrix can be reduced to blocks of fixed polarization, since $T_{ij}=0$ if $P_i\neq P_j$ (see, for instance, Ref. 3). The so-called central block is the one corresponding to zero polarization and describes a flat surface. The subcentral blocks (with polarization ± 2) describe surfaces with one step.

The difference between the free energies of a surface with a step and of a flat surface gives the step free energy, which, per unit of length, on an $N\times\infty$ strip can be expressed as

$$\beta f_S(N)=-[\ln\lambda_1(N)-\ln\lambda_0(N)], \tag{12}$$

where $\lambda_0(N)$ and $\lambda_1(N)$ are the largest eigenvalue of the central and the subcentral block, respectively.[30] The study of this quantity will allow us to determine the roughening temperature.

The deconstruction transition can be studied by considering two correlation lengths, which are both defined within the central block. We define the inverse correlation length ξ_D^{-1} as

$$\xi_D^{-1}(N)=-[\ln\lambda_2(N)-\ln\lambda_0(N)], \tag{13}$$

where $\lambda_2(N)$ is the second largest eigenvalue of the central block. The other correlation length can be calculated from the diagonal TM as the inverse of the domain-wall free energy per unit length $f_W^{-1}(N)$, where $f_W(N)$ is given by

$$f_W(N)=f(N)-\frac{f(N+1)+f(N-1)}{2} \tag{14}$$

with N odd. Indeed in the diagonal TM an $N\times\infty$ strip, with N odd, is partially frustrated since it cannot accommodate the Manhattan ground state without creating a domain wall (see Fig. 7). $f_W^{-1}(N)$ can be interpreted as the correlation length connected to the correlation function between two disorder variables.[31]

Conformal invariance[32] predicts that, at a critical point, the correlation lengths scale as N, so the deconstruction transition can be located at the crossing point of the curves representing the scaled quantities N/ξ_D and $N\beta f_W$ as functions of the temperature for different sizes. In reality, as shown in Figs. 8(a) and 8(b), no perfect crossing is found. Instead, pairs of curves obtained for sizes N and $N+2$ intersect each other in a sequence of points, $[\beta\delta_D(N),\beta\epsilon_D(N)]$, respectively $[\beta\delta_W(N),\beta\epsilon_W(N)]$, which converges to the infinite system critical point $(\beta\delta_D,\beta\epsilon_D)$, respectively $(\beta\delta_W,\beta\epsilon_W)$. An extrapolation procedure requiring several iterations[33] is then used to estimate $\beta\delta_D$ or $\beta\delta_W$. Of course the two independent estimates of the critical point have to coincide, which provides a good check on the internal consistency and accuracy of our procedures.

To locate the roughening temperature one has to employ a different method. The scaling $f_S(N)\sim 1/N$ holds not only at the KT transition but also inside the rough region, where the surface is in a critical state. There the curves $Nf_S(N)$, plotted as functions of temperature for different values of N, coalesce in the limit $N\to\infty$ and the point where they detach from each other can be identified as the KT point (see Fig. 9). For an accurate location of T_R one has to use the universal properties of the KT transition which give rise to the scaling prediction[12,34]

$$N\beta f_S(N)=\frac{\pi}{4}+\frac{1}{A+B\ln N}, \tag{15}$$

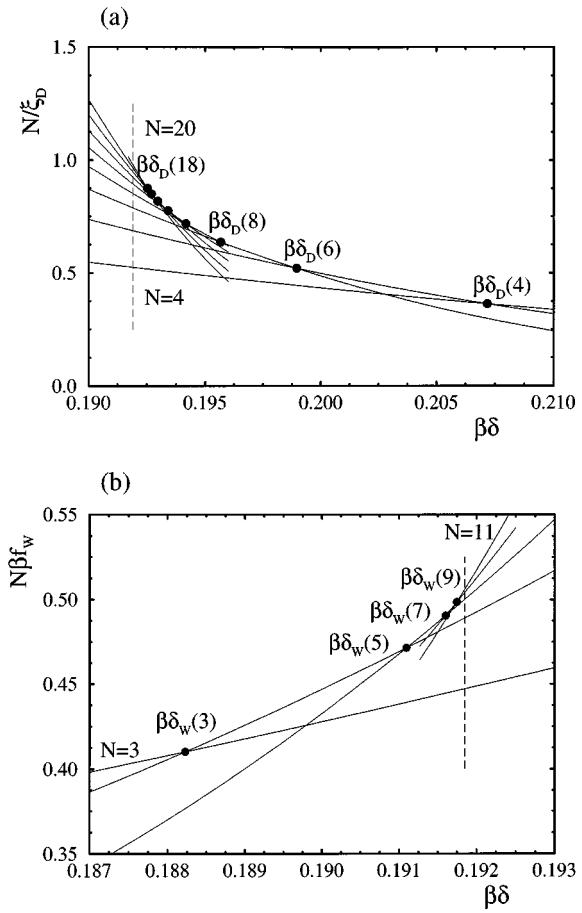

FIG. 8. The scaled correlation lengths $N\xi_D^{-1}(N)$ (a) and $N\beta f_W(N)$ (b) used to analyze the deconstruction transition by means of the vertical, respectively, the diagonal transfer matrix. The curves for different system sizes intersect in a sequence of points which for increasing N extrapolate to the deconstruction transition temperature. The figures refer to a scan along the thermal trajectory (Ref. 28) characterized by $\epsilon/\delta=-6.0$. The extrapolated values for (a) and (b) (dashed lines) coincide within error bars (not shown).

which holds exactly at $T=T_R$, with A and B nonuniversal constants. The constant $\pi/4$ is characteristic for steps with a height of two vertical lattice spacings. The free energy of such a step corresponds to the line tension between a vortex-antivortex pair with vorticity 2 in the dual representation.[12] The KT transition temperature is determined by requiring that a three-point fit of the form $N\beta f_S(N)=A_0+1/(A+B\ln N)$ yields $A_0=\pi/4$. For the extrapolation we used iterated fits in the spirit of Ref. 35. We performed this procedure along different lines across the phase diagram, scanning lines with $\beta\delta$ fixed, lines with $\beta\epsilon$ fixed, and thermal trajectories.[35]

V. CRITICAL EXPONENTS AND CENTRAL CHARGE

As we noted in the previous section, the critical line separating the flat from the rough region can be well characterized as a KT line. As we will see, the critical properties of the second-order line are less well determined, especially in the region $\epsilon'<0$. We will calculate critical exponents and central charge pertaining to the deconstruction transition us-

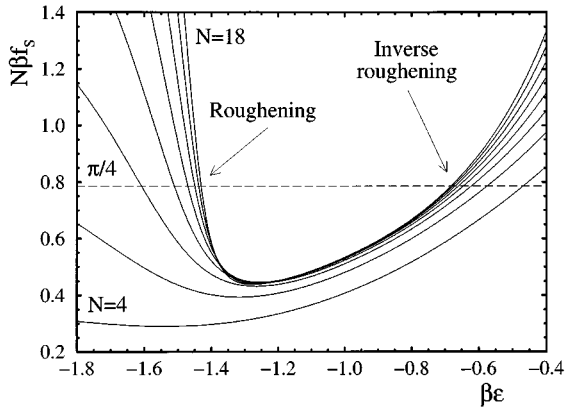

FIG. 9. The scaled step free energy $N\beta f_S(N)$ for different system sizes along a vertical scan across the phase diagram ($\beta\delta=0.14$). Coalescence of curves is an indication that the surface is in a rough state. Both the roughening transition and the inverse roughening transition are visible: they can be roughly localized in the regions where the curves approach the value $\pi/4$.

ing finite-size scaling methods. The two exponents α and ν are related to the behavior of the singular part of the surface free energy $f_{\rm sing}\sim t^{2-\alpha}$ and of the domain-wall free energy $f_W\sim t^{\nu}$ (Ref. 36) (where $t=(T-T_D)/T_D$, T_D the deconstruction temperature). They satisfy the finite-size scaling predictions

$$\frac{1}{N}\frac{\partial^2 f(N)}{\partial t^2}\sim N^{\alpha/\nu} \tag{16}$$

and

$$N\frac{\partial f_W(N)}{\partial t}\sim N^{1/\nu}, \tag{17}$$

respectively, valid at the critical point $T=T_D$. Two other critical indices we will calculate are

$$x=\frac{1}{2\pi}\lim_{N\to\infty}\frac{N}{\xi_D(N)}\bigg|_{T=T_D}, \tag{18}$$

$$x'=\frac{1}{2\pi}\lim_{N\to\infty}N\beta f_W(N)\bigg|_{T=T_D}, \tag{19}$$

which represent the exponent of the spin-spin correlation function[37] and that of the correlation function between disorder variables,[31] respectively. The numerical errors on the values assumed by these quantities are obtained as follows. We first evaluate the error on the determination of the critical temperature ΔT_D from the quality of the extrapolation to $N\to\infty$ of our finite-size data.[33] Subsequently, we extract the values of the exponents, again by iterated fits, at three different temperatures: $T_D-\Delta T_D$, T_D, and $T_D+\Delta T_D$. This procedure allows us to determine the maximum possible variation on the values of α/ν, ν, x, and x', thus assigning them an error bar. Notice these errors are typically small if the critical temperature is determined accurately enough.

Finally, from conformal invariance[32,38] it follows that the leading finite-size correction to the free energy per site of an

infinite system with periodic boundary conditions, $\tilde{f}_\infty$, is determined by the central charge (or conformal anomaly) c as

$$\frac{f(N)}{N} \approx \tilde{f}_\infty + \frac{\pi c}{6N^2}. \tag{20}$$

In fact we analyzed the central charge using the finite-size approximation

$$c(N,N+2) = \frac{3}{2\pi}\frac{N^2(N+2)^2}{(N+1)}\left(\frac{f(N)}{N} - \frac{f(N+2)}{N+2}\right) \tag{21}$$

which converges to c in the limit $N \to \infty$.

With the techniques described above we find that the deconstruction line for $\epsilon < 0$ belongs no doubt to the Ising universality class in sector B of our phase diagram. Good convergence with increasing size is obtained for the critical exponents as well as for the central charge, the values of which are

$$\alpha = 0, \quad \nu = 1, \quad x = x' = \frac{1}{8}, \quad c = \frac{1}{2}. \tag{22}$$

In the region $\epsilon' < 0$ the situation is less clear. The convergence of the data with increasing system size is worse, the values of some of the critical exponents seem to vary along the critical line and the central charge cannot be determined with any great accuracy. Yet our results seem to clearly rule out the possibility that the critical line remains in the Ising universality class. We present the results for the various exponents and for the central charge below and then draw some more general conclusions.

A. The exponent x

In part of sector C of the phase diagram we find difficulties in convergence for the quantities extracted from the correlation length $\xi_D(N)$. Figure 10(a) shows the behavior of the exponent x obtained from Eq. (18), only along part of the deconstruction line. The extrapolation procedure to infinite size is in fact far from trivial close to the horizon $\epsilon + 2\delta = 0$, where we find nonmonotonic behavior with increasing size for $N/\xi_D(N)$ and even for the sequence $\beta\delta_D(N)$. In order to give an estimate of the exponent x nonetheless, we looked at the quantity $x(N) \equiv N/[2\pi\tilde{\xi}_D(N)]$, where $\tilde{\xi}_D(N)$ is the correlation length evaluated now at the intersection points $[\beta\delta_D(N), \beta\epsilon_D(N)]$.

Figure 10(b) shows some plots of $x(N)$ vs N along the deconstruction line. The curves 1, 2, and 3 refer to critical points in sector B located on the deconstruction line at $\beta\delta = 0.88$, $\beta\delta = 0.60$, and $\beta\delta = 0.45$. They show a good convergence to the Ising exponent $x = 1/8$. The other curves, (4–10), refer to the values $\beta\delta = 0.37$, 0.31, 0.28, 0.25, 0.23, 0.21, 0.20, 0.19 in sector C of the phase diagram. As the system size increases the curves (4–7) show a reentrant behavior towards the value $x = 1/8$. At values of $\beta\delta \lesssim 0.20$ we find monotonic convergence again as function of system size, but to values which vary continuously as shown in Fig. 10(a). The behavior of this set of curves suggests that along any thermal scan in sector C of the phase diagram the quantity $x(N)$ will show an asymptotic decrease after a maximum. The position of the maximum gradually shifts to higher values of size until it exceeds the largest value accessible to our calculations and eventally disappears from sight. As already mentioned, no accurate fit can be performed on curves 4, 5, 6, and 7 of Fig. 10(a), though a rough estimate provides values of x below 1/8. When a fitted value can be extracted again (at smaller values of $\beta\delta$) and drawn in Fig. 10(a), one should thus be cautioned against the possibility of missing a maximum and a decreasing part. This would provide values of x possibly below 1/8 and more in accordance with those of x' given in the following subsection. However, another difficulty may arise: in the vicinity of the roughening transition the correlation length ξ_D may also be strongly influenced by steplike excitations.[39] A better quantity to look at is represented by the exponent x'.

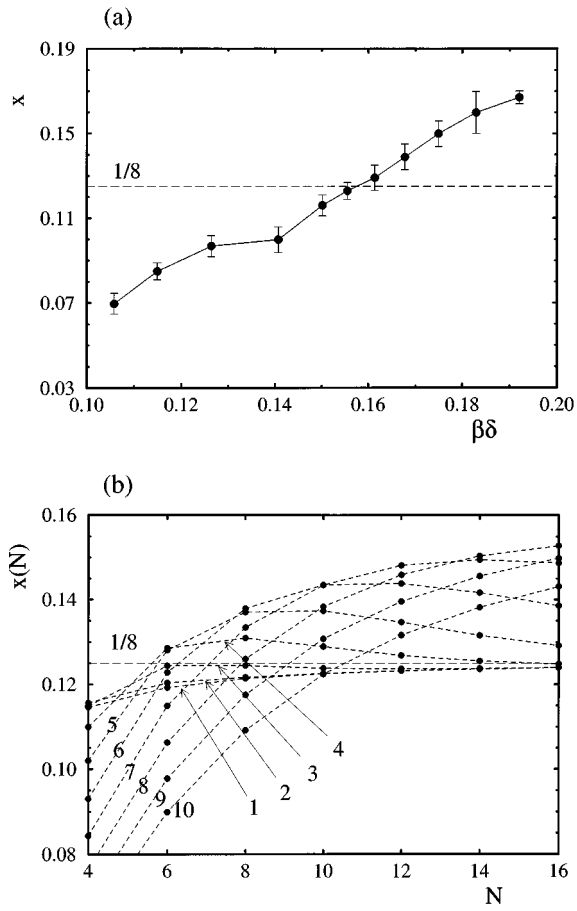

FIG. 10. (a) The exponent x calculated along the deconstruction line, in the range of values of $\beta\delta$ where the convergence is monotonic. (b) Nonmonotonic behavior of $x(N)$ as a function of N: curves 1, 2, and 3 refer to critical points in sector B of the phase diagram (and tend to the value 1/2), while all the other curves (4–10) refer to points in sector C (see text). For (4–10), due to the limitation in the maximum system size available (larger than that shown here) it is almost impossible to obtain a good extrapolation for $N \to \infty$.

B. The exponent x'

The quantity $N\beta f_W(N)$, converges monotonically as function of the system size N all along the deconstruction

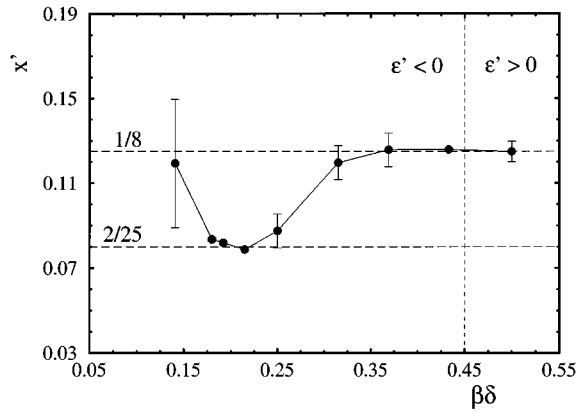

FIG. 11. The exponent x' calculated along the deconstruction line. The horizontal dashed lines represent the Ising value 1/8 and the four-state Potts exponent 2/25. Error bars smaller than the symbol size are not shown.

line. For $0.25 \lesssim \beta\delta \lesssim 0.40$ the convergence is slow, but it is still possible to give an estimate of the exponent x' using Eq. (19). However the error bars are fairly large. We notice a change in the direction of convergence: $N\beta f_W(N)/2\pi$ converges to x' from above in sector B of the phase diagram but from below in sector C. Around the line $\epsilon' = 0$ finite-size effects are very small. For $0.3 \lesssim \beta\delta \lesssim 0.4$ the exponent is still compatible, within error bars, with the Ising value of 1/8, as shown in Fig. 11, but for $\beta\delta \lesssim 0.3$ the exponent shifts towards values well below this.

C. The exponents α and ν

Figure 12 shows the exponents α and ν calculated with the diagonal transfer-matrix along the deconstruction line, with the aid of standard extrapolation methods based on the scaling relations (16,17).[40] It is almost impossible to obtain these exponents using the vertical transfer matrix, due to difficulties in convergence with increasing size. These problems are much less severe with the diagonal transfer matrix (see also the Appendix), even though the maximum available system size is smaller. The values thus obtained are not compatible with Ising exponents when $\epsilon' < 0$. They do satisfy the hyperscaling relation $2\nu = 2 - \alpha$ within error bars.

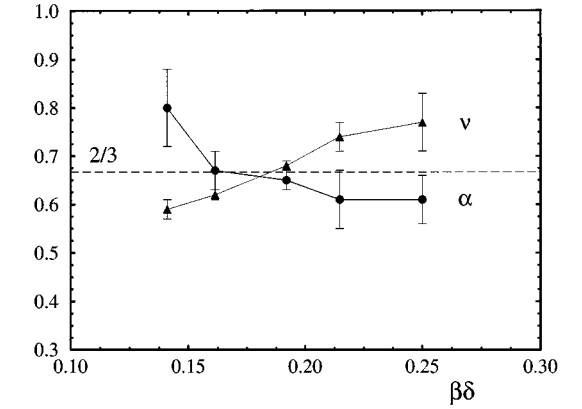

FIG. 12. The critical exponents α and ν calculated along the deconstruction line. The dashed line represents their value in the four-state Potts model.

D. The central charge

In general the central charge c vanishes in noncritical phases (here the flat reconstructed phase and the DOF phase) and assumes finite values at critical points or inside critical regions (like the rough phase). As in the determination of the exponents α and ν, c is calculated with the diagonal TM, as this leads to better convergence and smaller finite-size effects than calculations with the vertical TM. Figure 13(a) shows finite-size approximations of c along vertical lines in the phase diagram based on Eq. (21). The left part of Fig. 13(a) refers to a scan with $\beta\delta = 0.55$, which crosses the deconstruction line in a point of sector B, where we find exponents in the Ising universality class. In this case the central charge at the transition shows good convergence towards the Ising value ($c = 1/2$). The right part of Fig. 13(a) refers to a scan which crosses the deconstruction line in a point of sector C with $\beta\delta = 0.25$. Figure 13(b) shows two other plots of central charges along vertical lines with $\beta\delta = 0.22$ (left) and $\beta\delta = 0.20$ (right). In this part of the phase diagram the central charge increases markably beyond the Ising value $c = 1/2$. Due to strong finite-size effects, slow convergence and nearness of the KT line we cannot give a reasonable estimate for its actual value.

Figure 13(c) shows the central charge calculated along the thermal trajectory $\epsilon + 10\delta = 0$, starting from the rough region (at small $\beta\delta$) towards the reconstructed phase at larger $\beta\delta$. According to our numerical results the line $\epsilon + 10\delta = 0$ crosses the roughening and the deconstruction line in two points very close in temperature. In the infinite system limit the central charge should be 1 in the rough region, drop abruptly from 1 to 0 at the KT point, remain 0 in the DOF region, assume a nonzero value at the single point where the trajectory crosses the deconstruction line and remain 0 beyond that. In finite systems this behavior is smeared out, as is the case also in the other plots in Fig. 13. Hence, since the KT point and the deconstruction transition are extremely close on this trajectory, one expects to see an apparent convergence of c to the sum of the KT value 1 and that of the deconstruction transition. For a deconstruction of the Ising type this would yield $c = 3/2$. From conformal invariance[32] it follows that for unitary models with central charge smaller than unity c can only assume the values

$$c = 1 - \frac{6}{M(M+1)} \quad \text{with} \quad M = 3,4, \ldots . \tag{23}$$

The Ising value $c = 1/2$ is the lowest possible value, obtained with $M = 3$. Higher values of M correspond to phase transitions in different universality classes. From Fig. 13(c) it is apparent that c converges to a value larger than 3/2, which we estimate around $c = 1.7$–1.8.

E. Deconstruction of non-Ising type?

The results presented above strongly suggest that the deconstruction transition is not in the Ising universality class in, at least, part of the region $\epsilon' < 0$. One cannot entirely exclude the possibility that the observed deviations of critical

exponents and central charge from their Ising values are due to strong crossover effects, induced by the vicinity of the KT line,[39] rather than being a genuine feature of the deconstruction transition; in view of our numerical results however, we believe this is quite unlikely.

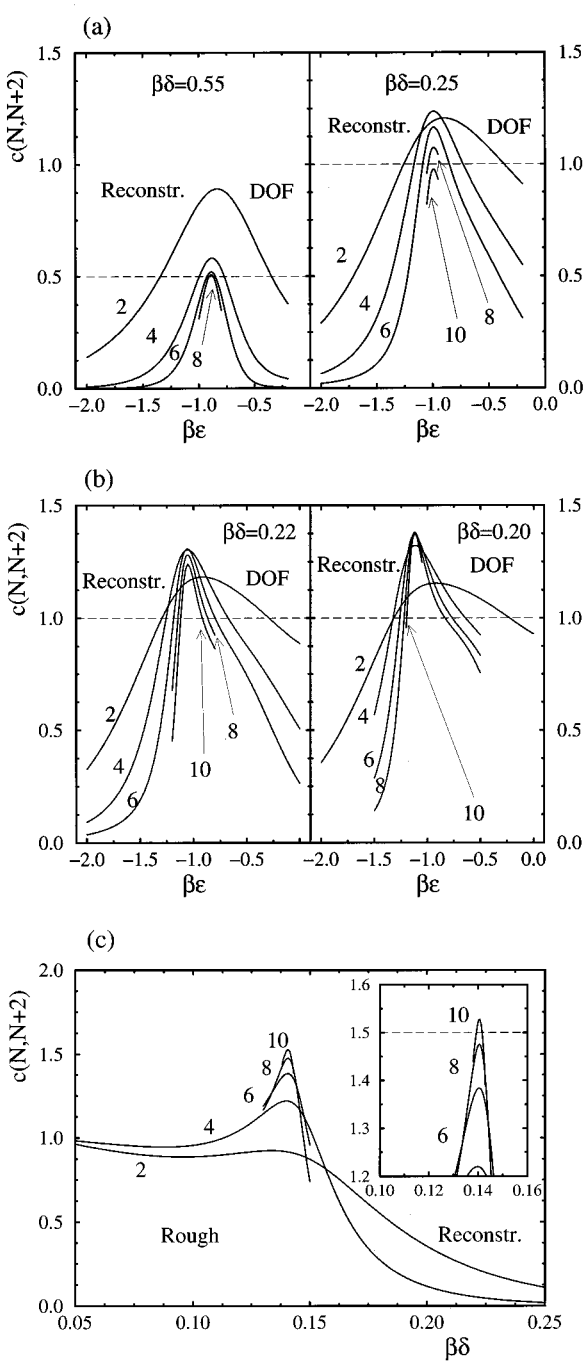

FIG. 13. Finite-size approximations $c(N,N+2)$ of the central charge from Eq. (22) (numbers denote the system size N) across different phases in the phase diagram calculated along vertical scans at [(a), left] $\beta\delta=0.55$, [(a), right] $\beta\delta=0.25$, [(b), left] $\beta\delta=0.22$, [(b), right] $\beta\delta=0.20$ and (c) along the thermal trajectory $\epsilon/\delta=-10.0$. The inset in (c) is just an enlargement of the same graph emphasizing the convergence of the central charge to values larger than 1.5.

Of course, the next intriguing question is: what, if not Ising, is the universality class of this reconstruction line? The answer to this question is not easy and our numerical results are not conclusive.

In general the exponents vary along the deconstruction line, although some vary less than others. The exponent x shows generally worse convergence than the exponent x' and extrapolation of the values of x in part of the phase diagram turned out impossible due to the nonmonotonic behavior of the finite-size data as a function of the system size N.

The exponent x' varies along the deconstruction line as well, but it remains roughly constant in a limited region around the value of $\beta\delta\approx 0.2$, with small error bars thanks to rapid convergence of the finite-size data. At smaller values of $\beta\delta$ its value increases as well as its error bars. This may be due to the vicinity of the KT line or to the finite-size effects caused by the increasing length of straight step segments. In general finite-size effects increase at smaller values of $\beta\delta$ (see also the Appendix); in this part of the phase diagram the most important excitations consist of closed loops of reversed arrows which may become very elongated as the energy per unit of length for a straight segment is proportional to 2δ. One should expect that finite-size effects are particularly strong when the typical size of a loop becomes of the same order of magnitude as the width of the strip, N. Slow convergence also is present in a region to the left of the line $\epsilon'=0$, as can be seen from the large error bars around $\beta\delta\approx 0.3$ in Fig. 11. This is due to a poor determination of the value of the deconstruction temperature T_D.

The exponents α and ν, as calculated from Eqs. (16),(17), vary along the deconstruction line in sector C. However, the hyperscaling relation $2\nu=2-\alpha$ is always satisfied within error bars. In general, as shown in Fig. 12, α tends to have larger error bars than ν. In the region $\beta\delta\approx 0.2$, the convergence is rapid in the sense that a two-parameter fit is sufficient to extract α and ν from Eqs. (16) and (17). At smaller values of $\beta\delta$ one, in general, needs to consider corrections to scaling using a three-parameter fit.

Unfortunately our numerical results do not allow an inequivocal identification of the critical behavior of the deconstruction transition in the region $\epsilon'<0$. We notice however that the exponent x' remains constant in a region around $\beta\delta\approx 0.2$, where the error bars are smallest. In this region also α and ν converge rapidly with increasing size, compared to other parts of the deconstruction line in sector C. One possible candidate for the observed exponents in this region could be that of the four-state Potts model, for which $\alpha=\nu=2/3$, compatible with our calculated values of α and ν.

Conformally invariant models are classified according to the value of their central charge, which can assume only discrete values depending on some integer M, as given in Eq. (23). At fixed values of M conformal invariance[32] predicts also the possible values for the exponents of correlation functions at the critical point. For the four-state Potts model, the predicted exponents are of the type $x,x'=2p^2/q^2$ with p and q integers, as pointed out in Ref. 41. For $p=1$ and $q=4$ one indeed obtains the well-known magnetic exponent 1/8, instead for $p=1$, $q=5$ one obtains the value 2/25. Both values are shown as horizontal dashed lines in Fig. 11; the

exponent $x'=2/25$ seems to fit the measured values of the exponent very well for $\beta\delta\approx 0.2$. For the two-dimensional Ising model conformal invariance predicts the exponents $x=1/8$ (magnetic) and $x=1$ (thermal) only. Thus a measured exponent of value $x'\approx 2/25$ is a quite clear sign of non-Ising critical behavior.

Further, the central charge clearly shifts away from its Ising value $c=1/2$. For the four-state Potts model we should expect a central charge equal to 1 [$M\to\infty$ in Eq. (23)]. The central charge markably increases in the region $\epsilon'<0$. However, as for the critical exponents, this increase goes smoothly from the Ising value, $c=1/2$, towards higher values. The central charge calculated along the line $\epsilon+10\delta=0$, where the deconstruction and roughening line are almost coinciding in temperature, extrapolates to $c=1.7-1.8$, well above the Ising plus KT value $c=1/2+1=3/2$. As pointed out above, this is another indication of non-Ising behavior of the deconstruction transition, though not quite compatible with that of the four-state Potts model, which would imply a central charge equal to $c=1+1=2$.

Finally, also the possibility of having a line with continuously varying exponents, as the behavior of especially the exponent x in the sector C suggests [Fig. 10(a)], should be considered. In this case the central charge would equal unity, as in the four-state Potts model.

Anyhow, as discussed in Secs. V A and V B, the convergence of x is much poorer than that of x'. The slow shift of x' away from the Ising value as $\beta\delta$ decreases in sector C (Fig. 11) is known to be a common feature of finite-size scaling in the vicinity of points where a change of universality class occurs. Moreover, as $\beta\delta$ becomes very small, the nearness of the KT line is seen to influence the convergence of the exponents of the deconstruction line. In conclusion, it seems quite plausible to have in practice only a window of $\beta\delta$ values where constant critical exponents are found. To enlarge this window one would have to consider larger system sizes.

Bastiaansen and Knops[11] recently studied a six vertex model with an extended range of interactions. They also found a phase diagram with a second-order line approaching a KT line. The exponents of the second-order line clearly deviate from their Ising values and the authors suggested they might be explained as tricritical Ising exponents. Applied to the staggered BCSOS model this would mean a deconstruction line of Ising type with a tricritical point, continuing beyond this point as a first order line, which is the phase behavior of the annealed diluted Ising (or Blume-Capel[42]) model. The exponents at the tricritical point would be $\alpha=8/9$, $\nu=5/9$, and the central charge $c=7/10$. For the exponent x' conformal invariance predicts $x'=3/40$. Around $\beta\delta\approx 0.2$ the extrapolated value of x' would also be compatible with this value, but α and ν are far away from their tricritical values. At smaller values of $\beta\delta$ we do find exponents which approach those of the tricritical Ising model, but this happens in a region where the values we obtain for x' clearly shift away from 3/40 and where in general finite-size effects are quite strong. These same finite-size effects also make it impossible to tell whether at sufficiently small $\beta\delta$ the deconstruction line becomes first order or not.

The point along the deconstruction line where the change of universality class occurs is not sharply determined by our numerical results. We do not observe an abrupt jump of the exponents at a given point, rather a continuous shift. A reasonable candidate for the point separating the two regions (i.e., Ising and non-Ising), could be the point where the deconstruction line crosses the line $\epsilon'=\epsilon+2\delta=0$. Crossing this line, we find changes in the type of convergence of the exponents x and x' (Secs. V A and V B), although without an abrupt change in their values. We recall that in the surface representation of the model, in one region the coupling constants between the atoms in the two sublattices are both negative ($\epsilon<0$, $\epsilon'<0$); in the other (where the deconstruction transition is of Ising type) one of the two coupling constants is positive ($\epsilon'>0$). In terms of the vertex lattice, in the region $\epsilon'>0$, vertices 5 and 6 are the excited vertices with the lower energy above the ground-state value; at $\epsilon'<0$, vertices 5 and 6 get the higher excitation energy.

All these considerations suggest that the properties of the system may change between the two regions $\epsilon'>0$ and $\epsilon'<0$ and make it more plausible that the shifts in the exponents are not just due to crossover, but also result from a real change of universality class of the deconstruction transition.[43]

VI. DISCUSSION AND CONCLUSION

In this article we studied the critical properties of the staggered BCSOS model. Using transfer-matrix techniques we found two critical lines describing the deconstruction and the roughening of the (001) surface of a two-component bcc crystal.

The two lines approach each other in part of the phase diagram, apparently without merging. According to our results the deconstruction line in part of the phase diagram changes its universality class from Ising to non-Ising, although further investigations are needed to make this point more convincing. On the basis of the exponents we find, we conclude that a possible universality class matching these exponents reasonably well, in the region where the best convergence is found, is that of the four-state Potts model. Another possible scenario is that proposed by Bastiaansen and Knops.[11] In their six vertex model with interactions extended to further neighbors it is too hard to distinguish between a single critical line and two lines approaching each other, but remaining separate. They find critical exponents for the deconstruction transition clearly deviating from the Ising values and conjecture that the observed criticality could be explained as tricritical Ising behavior. The idea of a diluted Ising model is particularly attractive in our case where, as we have seen, the deconstruction transition is, to all likeliness, the consequence of the dilution of the Ising order in the system caused by the formation of a large number of closed steps of finite length. Unfortunately we find little numerical evidence for this scenario. Finally, also the possibility of having a line with continuously varying exponents cannot be completely excluded. Other models of reconstructed surfaces have been studied by several authors. Den Nijs[16] introduced a model that describes (110) missing-row reconstructed surfaces of some fcc metals (Au,Pt, . . .). He found a deconstruction and a roughening line merging into a single critical

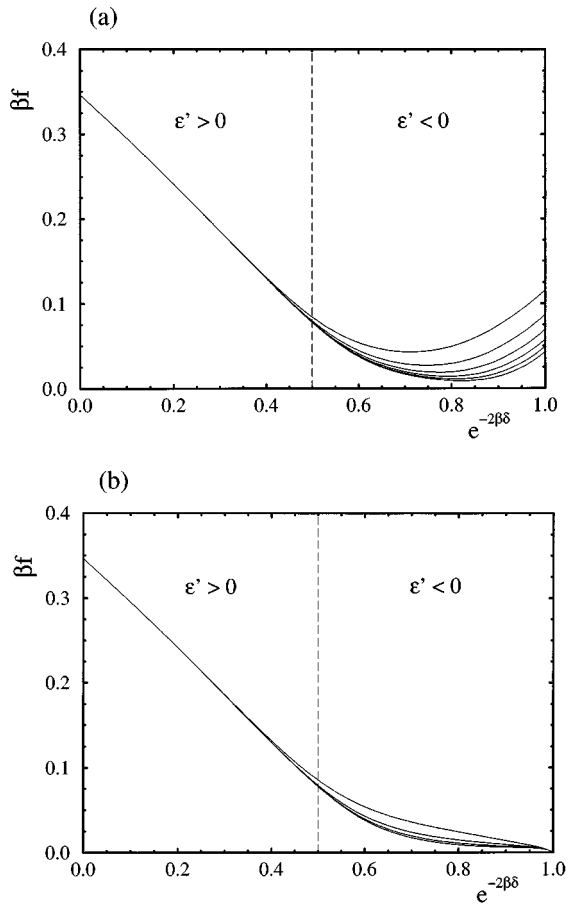

FIG. 14. Free energy along the line $e^{\beta\epsilon}+e^{-2\beta\delta}=1$ [Eq. (9)] calculated (a) with the vertical transfer matrix and (b) with the diagonal transfer matrix for different system sizes. Notice the different scaling behavior especially at the point $e^{-2\beta\delta}=1$: in (a) the curves for increasing N tend to the infinite system size value (zero) like $\ln 2/N$, in (b) they *are* zero. It is apparent that finite-size effects are generally smaller in (b).

line, with Ising and KT behavior simply superimposed. From his data, as presented in the literature, it is not possible to really distinguish between actual merging or mere rapid approach of the lines. A clear distinction to our model is that in Den Nijs' model the deconstruction transition remains Ising type throughout. Another class of models for the same metal surfaces has been developed and extensively studied by the Trieste group.[10,44] Again a deconstruction line and a KT roughening line are seen to approach each other. Depending on the microscopic details of the model, the deconstruction line keeps its Ising character either all along, or up to a tricritical point where it changes to a first-order line.

As mentioned in the Introduction there are several other two-dimensional models with KT and Ising degrees of freedom. One that has received a lot of attention, starting from the beginning of the last decade,[45] is the fully frustrated XY model, which describes certain two-dimensional Josephson-junction arrays. The study of its critical behavior has led to several different conjectures about its universality class and critical exponents. Several papers[17,18] report non-Ising exponents and it has been suggested that the model would belong to a novel type of universality class. To our knowledge, whether this type of universality class would or

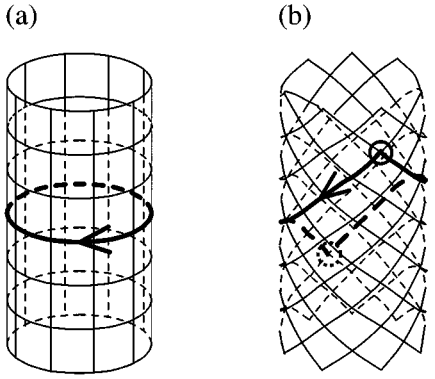

FIG. 15. When $\delta \ll \epsilon$, finite-size effects may show up in the form of closed loops of reversed arrows winding around the cylinder. In the diagonal transfer matrix (b) however they are less frequent than in the vertical transfer matrix (a) since they require at least one couple of vertices 5 and 6 (circles) for closing up the lace.

would not coincide with that of some known models has not been established yet. In the most recent study concerning the fully frustrated XY model, Olsson[19] presents evidence of two separate transitions, a KT and an Ising one where the former occurs at somewhat lower temperature than the latter: $T_{\mathrm{KT}}<T_{\mathrm{IS}}$. This would be in agreement with our results since the XY model can be mapped onto a solid-on-solid model via a duality transformation,[46] which maps the low-temperature phase of one model onto the high-temperature phase of the other and vice versa. Olsson's work suggests that the non-Ising exponents observed by other groups are due to the failure of some finite-size scaling hypothesis used in previous works. In the staggered BCSOS model instead, we find clear evidence of non-Ising exponents. Unfortunately there exists no exact mapping between this model and the fully frustrated XY model, therefore they may well be in different universality classes. Yet, we hope that some of the ideas developed in this paper to study the staggered BCSOS model, will be generalized to other models so as to reach a deeper understanding of their critical properties.

ACKNOWLEDGMENTS

It is a pleasure to thank Paul Bastiaansen, Henk Blöte, Hubert Knops, Bernard Nienhuis, and Marcel den Nijs for stimulating discussions. Financial support permitting several meetings between the authors of this paper is gratefully acknowledged. In particular H.v.B. thanks the Centro di Fisica delle Superfici e delle Basse Temperature (CNR), Genova, while G.M. thanks the Instituut voor Theoretische Fysica, Utrecht, and acknowledges the kind hospitality of Professor Dietrich Wolf at HLRZ, Jülich.

APPENDIX: FINITE-SIZE EFFECTS

We show here how the diagonal and the vertical transfer matrix have different finite-size effects in part of the phase diagram. Consider first the phase point $\delta=0$, $\epsilon\to-\infty$. Vertices 5 and 6 are absent and the partition function can be calculated easily. Consider lattices of size $N\times M$ with cylindrical geometry, that is the N vertices along a horizontal row are connected to each other through periodic boundary con-

ditions. In the vertical transfer matrix there are in total 2^{N+M} configurations, and the free energy per site is given by

$$-\beta\tilde{f}=\frac{N+M}{NM}\ln 2 \tag{A1}$$

(the symbol $\tilde{f}$ is used to distinguish the free energy per site from f, the free energy per row). In the thermodynamic limit $N,M\to\infty$ the free energy per site vanishes.

However in transfer-matrix calculations one takes the limit $M\to\infty$ keeping N finite; this gives a free energy per site equal to

$$-\beta\tilde{f}=\frac{1}{N}\ln 2. \tag{A2}$$

With the diagonal transfer matrix the total number of configurations available is 2^{2N}, since once the arrows on a row are fixed the whole configuration is fixed. Repeating the same calculation as done above one finds a free energy per site:

$$-\beta\tilde{f}=0 \tag{A3}$$

independent of the value of N. The conclusion is that the free energy shows finite-size corrections of the order $1/N$ in the vertical transfer matrix, while there are no finite-size effects for the diagonal transfer matrix. In Fig. 14 we plot the free energy calculated along the line $e^{\beta\epsilon}+e^{-2\beta\delta}=1$ with the vertical and diagonal transfer matrices. The endpoint $e^{-2\beta\delta}=1$ corresponds to the free energy which we calculated in Eqs. (A1) and (A3). As can be seen from the figure, there is a wide area to the left of this point where the free energies calculated from the vertical transfer-matrix show large finite-size effects, while the convergence is much faster for the diagonal transfer-matrix. In both cases the convergence is faster for $e^{-2\beta\delta}<1/2$, that is in the region of the phase diagram where only a second-order line is present. Obviously, for small values of δ the boundary effects are very strong, due to closed loops of reversed arrows winding around the cylinder, i.e., the ribbon which constitutes our system with periodic boundary conditions in the horizontal direction (see Fig. 15). These closed loops are more frequent in the vertical transfer matrix, since one can reverse the arrows along a horizontal line with a cost in energy of $2\delta N$. Closed loops in the diagonal transfer matrix require at least a vertex 5 and a vertex 6, and therefore occur less frequently.

*Present address: Instituut voor Theoretische Fysica, Katholieke Universiteit Leuven, Celestijnenlaan 200D, B-3001 Leuven, Belgium.

[1] J. C. Slater, J. Chem. Phys. **9**, 16 (1941).
[2] E. H. Lieb and F. Y. Wu, in *Phase Transitions and Critical Phenomena*, edited by C. Domb and M. S. Green (Academic, London, 1972), Vol. 1, pp. 331–490.
[3] R. J. Baxter, *Exactly Solved Models in Statistical Mechanics* (Academic, London, 1982).
[4] H. van Beijeren, Phys. Rev. Lett. **38**, 993 (1977).
[5] H. van Beijeren and I. Nolden, in *Structure and Dynamics of Surfaces*, edited by W. Schommers and P. von Blanckenhagen (Springer-Verlag, Berlin, 1987), Vol. 2, pp. 259–300.
[6] S. T. Chui and J. D. Weeks, Phys. Rev. B **14**, 4978 (1976).
[7] R. J. Baxter, Phys. Rev. B **1**, 2199 (1970).
[8] F. Y. Wu and K. Y. Lin, Phys. Rev. B **12**, 419 (1975).
[9] A. C. Levi and M. Touzani, Surf. Sci. **218**, 223 (1989).
[10] G. Mazzeo, G. Jug, A. C. Levi, and E. Tosatti, Phys. Rev. B **49**, 7625 (1994).
[11] P. J. M. Bastiaansen and H. J. F. Knops, Phys. Rev. B **53**, 126 (1996).
[12] E. Luijten, H. van Beijeren, and H. W. J. Blöte, Phys. Rev. Lett. **73**, 456 (1994).
[13] J. Ashkin and E. Teller, Phys. Rev. **64**, 178 (1943).
[14] H. J. F. Knops, Phys. Rev. B **20**, 4670 (1979).
[15] G. Mazzeo, E. Carlon, and H. van Beijeren, Phys. Rev. Lett. **74**, 1391 (1995); Surf. Sci. **352-354**, 960 (1996).
[16] M. den Nijs, Phys. Rev. Lett. **66**, 907 (1991); Phys. Rev. B **46**, 10 386 (1992).
[17] G. Ramirez-Santiago and J. V. José, Phys. Rev. Lett. **68**, 1224 (1992).
[18] Y. M. M. Knops, B. Nienhuis, H. J. F. Knops, and H. W. J. Blöte, Phys. Rev. B **50**, 1061 (1994).
[19] P. Olsson, Phys. Rev. Lett. **75**, 2758 (1995).
[20] E. Granato and J. M. Kosterlitz, Phys. Rev. B **33**, 4767 (1986).
[21] E. Granato, J. M. Kosterlitz, J. Lee, and M. P. Nightingale, Phys. Rev. Lett. **66**, 1090 (1991).
[22] E. H. Lieb, Phys. Rev. Lett. **18**, 1046 (1967).
[23] Crystallographically CsCl has a simple cubic structure; however, if one ignores the identities of the different ions one obtains a bcc lattice.
[24] F. Y. Wu and K. Y. Lin, J. Phys. C **7**, L181 (1974); H. J. F. Knops, J. Phys. A **8**, 1508 (1975); S. E. Ashley, *ibid.* **11**, 2015 (1978).
[25] T. Ohta and K. Kawasaki, Prog. Theor. Phys. **60**, 365 (1978).
[26] R. W. Youngblood and J. D. Axe, Phys. Rev. B **23**, 232 (1981).
[27] K. Rommelse and M. den Nijs, Phys. Rev. Lett. **59**, 2578 (1987); M. den Nijs and K. Rommelse, Phys. Rev. B **40**, 4709 (1989).
[28] M. Kohmoto, M. den Nijs, and L. P. Kadanoff, Phys. Rev. B **24**, 5229 (1981).
[29] In the diagonal transfer-matrix $N_{i\uparrow}$ and $N_{i\downarrow}$ refer to the number of arrows with vertical components pointing up or down, respectively.
[30] The largest eigenvalue of the transfer-matrix is always found in the central block.
[31] L. P. Kadanoff and H. Ceva, Phys. Rev. B **3**, 3918 (1971).
[32] J. L. Cardy, in *Phase Transitions and Critical Phenomena*, edited by C. Domb and J. L. Lebowitz (Academic, London, 1987), Vol. 11, pp. 55–126.
[33] H. W. J. Blöte and B. Nienhuis, J. Phys. A **22**, 1415 (1989).
[34] H. W. J. Blöte and P. Nightingale, Phys. Rev. B **47**, 15 046 (1993).
[35] The thermal trajectories are those trajectories in the phase diagram obtained by fixing the values of the energies and varying the temperature.
[36] With ν we indicate both the exponent of the correlation length ξ and of the interface free energy f_W. We recall that the general scaling hypothesis predicts that for all systems near the critical point $f_W\xi\sim k_BT$ holds. For more details the reader may consult B. Widom, J. Chem. Phys. **43**, 3892 (1965) and **43**, 3898 (1965), and D. B. Abraham, Phys. Rev. B **19**, 3833 (1979). In Ref. 15 we adopted ξ_D to extract ν, here better convergence is achieved by using f_W, anyway the finite-size scaling analysis on these

two different quantitites lead to the same estimate for ν when they both converge.

[37] The exponent x is related to the more standard exponent η as $x = \eta/2$.

[38] H. W. J. Blöte, J. L. Cardy, and M. P. Nightingale, Phys. Rev. Lett. **56**, 742 (1986); I. Affleck, *ibid.* **56**, 746 (1986).

[39] M. den Nijs (private communication).

[40] M. P. Nightingale, J. Appl. Phys. **53**, 7927 (1982).

[41] B. Nienhuis and H. J. F. Knops, Phys. Rev. B **32**, 1872 (1985), and references therein.

[42] M. Blume, Phys. Rev. **141**, 517 (1966); H. W. Capel, Physica **32**, 966 (1966).

[43] Of course, if the second scenario, of a diluted Ising line, would apply, the tricritical point is far removed from the point $\epsilon' = 0$ and there would have to be strong crossover effects.

[44] G. Santoro and M. Fabrizio, Phys. Rev. B **49**, 13 886 (1994); G. Santoro, M. Vendruscolo, S. Prestipino, and E. Tosatti, *ibid.* **53**, 13 169 (1996).

[45] S. Teitel and C. Jayaprakash, Phys. Rev. B **27**, 598 (1983).

[46] H. J. F. Knops, Phys. Rev. Lett. **39**, 766 (1977).